Hyperfine Interact
DOI 10.1007/s10751-016-1313-6

Iron films deposited on porous alumina substrates

Yasuhiro Yamada[1] · **Kenichi Tanabe**[1] ·
Naoki Nishida[1] · **Yoshio Kobayashi**[2,3]

Abstract Iron films were deposited on porous alumina substrates using an arc plasma gun. The pore sizes (120 – 250 nm) of the substrates were controlled by changing the temperature during the anodic oxidation of aluminum plates. Iron atoms penetrated into pores with diameters of less than 160 nm, and were stabilized by forming γ-Fe, whereas α-Fe was produced as a flat plane covering the pores. For porous alumina substrates with pore sizes larger than 200 nm, the deposited iron films contained many defects and the resulting α-Fe had smaller hyperfine magnetic fields. In addition, only a very small amount of γ-Fe was obtained. It was demonstrated that the composition and structure of an iron film can be affected by the surface morphology of the porous alumina substrate on which the film is grown.

Keywords Iron film · Porous alumina · Gamma-iron · Alpha-iron

1 Introduction

The properties of thin iron films are affected by the surface morphology of the films and their substrates. We previously demonstrated that when an aluminum foil with 100-nm grooves was employed as a substrate, the surface of the iron film also contained grooves.

This article is part of the Topical Collection on *Proceedings of the 2nd Mediterranean Conference on the Applications of the Mössbauer Effect (MECAME 2016), Cavtat, Croatia, 31 May-3 June 2016*

✉ Yasuhiro Yamada
yyasu@rs.kagu.tus.ac.jp

[1] Tokyo University of Science, 1-3 Kagurazaka, Shinjuku-ku, Tokyo 162-8601, Japan

[2] The University of Electro-Communications, 1-5-1 Chofugaoka, Chofu, Tokyo 182-8585, Japan

[3] RIKEN, 2-1 Hirosawa, Wako, Saitama 351-0198, Japan

Furthermore, the nuclear spin orientation of the iron tended to be linear along the grooves [1]. The energy of the evaporated iron atoms is also important to control the orientation of the iron lattice structure [2]. An arc plasma gun is an adequate tool for depositing iron films that reflect the morphology of the substrate. In this study, iron films were prepared on porous alumina substrates, and the effects of pore size were investigated using Mössbauer spectroscopy.

Porous anodic alumina films have attracted considerable attention in the field of nanotechnology, because they have a nanoscale porous structure. The pores are produced over a wide area of the aluminum surface, and the surface structure contains a huge number of nanoscale holes. The formation mechanism of porous alumina has been studied extensively [3]. The morphology of porous alumina on an aluminum film can be controlled by an appropriate selection of the electrolyte and film-forming conditions. Furthermore, porous alumina has been used as a template for producing nanomaterials. The preparation of Ni, Co, and Fe nanowires using an electrochemical method has been reported [4]. Lepidocrocite γ-FeOOH nanowire arrays in alumina pores were produced by electrodeposition [5]. Iron particles dispersed in a porous alumina host have been prepared by wet impregnation of $Fe(NO_3)_3$ and subsequent heat treatment in hydrogen [6]. The products were Fe/Al_2O_3 composites containing iron particles.

The direct deposition of Fe atoms on porous alumina has not yet been reported. We previously attempted to produce iron films on porous alumina using pulsed laser deposition (PLD), but smooth α-Fe films were formed on the substrate regardless of the pore size. As PLD produces high density Fe vapor, the Fe atoms did not penetrate into the pores but instead formed an α-Fe film covering the pores.

2 Experimental

Porous alumina was produced by anodic oxidation. An aluminum sheet (40 μm thick) and a carbon rod were employed as electrodes. The anodization was conducted at 60 V for 60 min in a phosphoric acid solution (0.3 M) at various temperatures between 15 and 30 °C, and the average resulting pore diameters were 160 to 250 nm. Arc deposition of iron was performed using an arc plasma gun (APG, ULVAC ARL-300) in vacuum. The thickness of the iron films was controlled by changing the number of pulses and the distance between the substrate and the APG. The amount of iron in the sample was estimated by weighing the sample before and after deposition, and the typical deposition rate of iron atoms using the APG was 0.01 to 0.16 nm/pulse. The deposition was performed for between 1000 and 18000 pulses. The surface morphology and pore size were observed by scanning electron microscopy (SEM, JEOL JSM-7001FSHL). X-ray diffraction (XRD, Rigaku RINT2500) patterns were measured to confirm the assignments, and Mössbauer spectra were measured in a transmission geometry using a ^{57}Co/Rh source.

3 Results and discussion

3.1 Thickness of the substrate

First, we examined the effects of the thickness of the iron film deposited on porous alumina. The surface morphology might have stronger effects when the thickness is small, but too little iron would hinder the spectroscopic measurements. Therefore, we attempted to

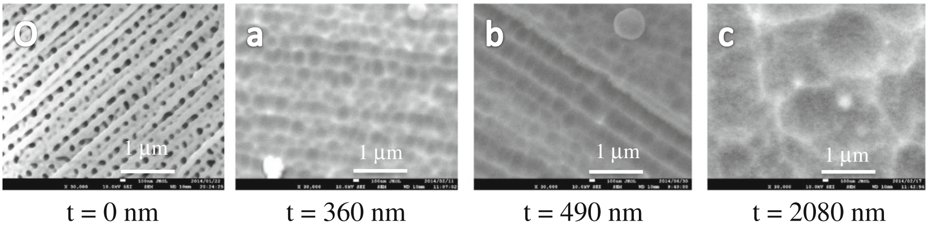

Fig. 1 SEM images of the surface of (O) the porous alumina substrates and iron films. Before deposition, the pores in the porous alumina substrate were 120 nm in diameter. The equivalent thicknesses of the films to those of α-Fe were (**a**) 360 nm, (**b**) 490 nm, and (**c**) 2080 nm

determine the adequate thickness at which to observe the effects of the substrate surface morphology.

SEM images Porous alumina produced at 15 °C had 120-nm-diameter pores; an SEM image of this porous alumina is shown in Fig. 1. Before the anodic oxidation, the aluminum plate contained nanosized grooves produced by rolling, and the pores tended to align along the grooves. The pores were not connected to each other, and the flat surface could be observed between the pores. We deposited iron atoms using APG, varying the thickness of the resulting iron films. When the equivalent thickness of deposited Fe to those of α-Fe was 360 nm, the pores were covered with iron but the surface morphology still reflected the pores in the substrate. When more iron was deposited and thicker films were produced (490 nm; Fig. 1b and 2080 nm; Fig. 1c), the surfaces of the iron films became smoother without reflecting the pores on the substrate surface.

Mössbauer spectra Mössbauer spectra of iron films deposited on porous alumina were measured at room temperature (Fig. 2). The Mössbauer spectrum of an iron film with 360 nm equivalent thickness was fitted into a combination of a singlet and a sextet (Fig. 2a). The sextet was clearly assigned to α-Fe from the Mössbauer parameters ($\delta = 0.0$ mm/s, $\Delta E_Q = 0.0$ mm/s, $H = 33.0$ T, Area intensity 83 %). The intensity ratio of the sextet was 3:3.4:1:1:3.4:3, indicating that the magnetic orientation was almost parallel to the substrate surface. Magnetic anisotropy caused by the shape anisotropy of the bcc-Fe lattice was observed in the thin film.

The singlet absorption observed in Fig. 2a was assigned to γ-Fe ($\delta = 0.0$ mm/s, Area intensity 17 %). Generally, γ-Fe is stable only at high temperatures and is unstable at room temperature. However, γ-Fe is reportedly stabilized in nanosized particles [7] and thin films [8, 9] at low temperatures. In this study, it is speculated that iron atoms penetrated into the nanosized pores, and the lattice formation within a tiny volume enhanced the production of γ-Fe. The singlet absorption may also appear when an Fe atom is isolated in an Al substrate, but the isomer shift of such an atom was reported to be $\delta = 0.4$ mm/s [10], too large for the singlet observed in the present experiments. It was reported that Fe atoms produced by PLD have a high energy (several hundred eV), and will migrate into an Al substrate [11]. In our previous studies on the deposition of Fe atoms on Al substrates using APG [1], we reported that α-Fe was the only product because the Fe atoms did not have sufficient energy to implant into the Al substrate. Therefore, the singlet was assigned to γ-Fe.

When the thickness was increased to 490 nm (Fig. 2b), the Mössbauer spectrum still consisted of α-Fe and γ-Fe, and the relative intensity of α-Fe increased to 95 %. The Mössbauer

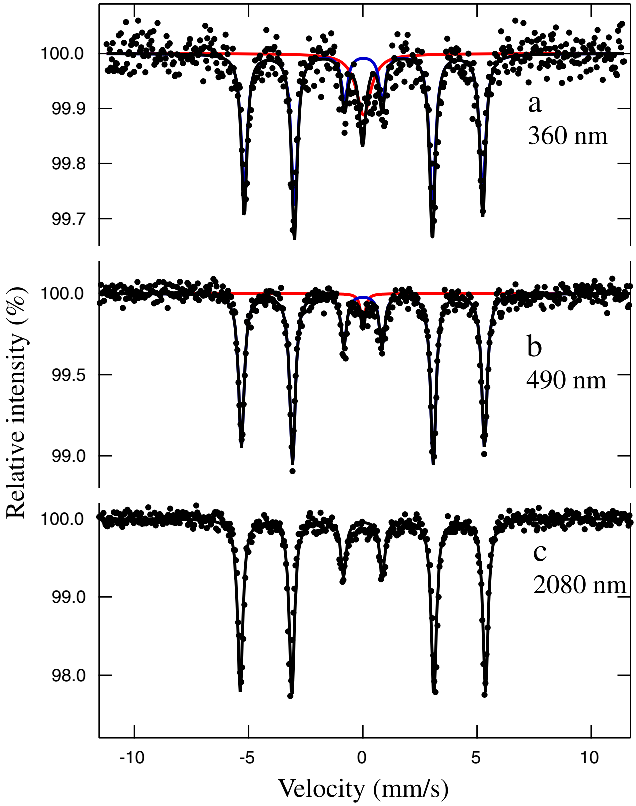

Fig. 2 Mössbauer spectra of iron films deposited on porous alumina substrates with 120-nm-diameter pores. The equivalent thicknesses of the iron films were (**a**) 360 nm, (**b**) 490 nm, and (**c**) 2080 nm

spectrum of the thickest sample (2080 nm thick) had only the absorption of α-Fe. This indicates that γ-Fe was produced only in the pores, and α-Fe formed over the pore openings to form a smooth surface.

XRD pattern The XRD pattern of a 360-nm-thick sample was measured (Fig. 3). The peaks were assigned using the AtomWorks database [12]. The intense peaks at 44.67°, 65.02°, and 82.34° corresponded to α-Fe, which overlapped with the Al peaks. The peak at 50.46° corresponded to γ-Fe. γ-Fe also has a peak at 43.33°, but this peak overlapped with the intense peak of α-Fe at 44.67°. In addition to these peaks, the sharp peak at 78.22° corresponded to Al, and no patterns corresponding to Al_2O_3 were observed. The production of γ-Fe was confirmed by the XRD pattern.

3.2 Pore size of the porous alumina substrate

It was shown that the α-Fe film became dominant when the thickness of the films became sufficiently large, and the resulting film did not reflect the surface morphology of the porous alumina substrate. In order to investigate the properties of the iron reflecting the surface morphology, we had to study thinner iron films. We produced 150-nm-thick iron films on

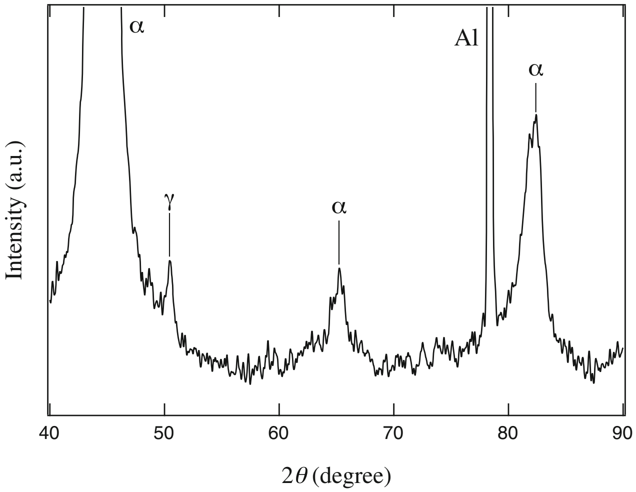

Fig. 3 XRD pattern of an iron film (360 nm thick) deposited on porous alumina with 120-nm-diameter pores

porous alumina substrates with different pore diameters ($d = 160$, 200, and 250 nm), in order to examine the effects of substrate pore size on the composition of the iron films.

SEM images SEM images of three porous alumina substrates with different pore diameters are shown in Fig. 4a1, b1, and c1. The films with smaller pore diameters had flat surfaces, as the distance between the pores was larger than the pore diameter (Fig. 4a1). On the other hand, films with larger pore diameters had almost no flat surface, as the distance between the pores and their diameters were almost the same, and the pores were connected to each other (Fig. 4b1 and c1). Iron films having 150 nm equivalent thickness were deposited using APG onto the porous alumina substrates. SEM images of the surfaces of the iron films were observed (Fig. 4a2, b2, and c2), and the surface of the iron films reflected the surface morphology of the porous alumina substrates. In order to observe the cross-sections of the pores, a crack was made in the sample shown in Fig. 4a2 and an SEM image of the resulting cross section of the iron film deposited on porous alumina is shown in Fig. 5. It can be seen that the Fe atoms penetrated $\sim$100 nm into the pores from the openings.

Mössbauer spectra Room-temperature Mössbauer spectra of iron films deposited on porous alumina substrates are shown in Fig. 6, and the Mössbauer parameters are summarized in Table 1. The Mössbauer spectrum of the iron film deposited on porous alumina with 160-nm-diameter pores (Fig. 6a) was fitted as a combination of a sextet and a singlet, which were respectively assigned to α-Fe and γ-Fe. The γ-Fe yield of this sample (28 %) was higher than that of the iron film shown in Fig. 2a (17 %), mainly because the iron film was thinner and less α-Fe covered the pores or the planar regions of the substrate surface. The iron film stacked on the flat surface of the substrate formed the α-Fe lattice, whereas the iron atoms penetrating into the nanosized pores became γ-Fe. A Mössbauer spectrum of the same sample was measured at low temperature (6 K), and the spectrum shape remained unchanged, showing the same singlet.

When the substrate had larger pores (200 nm; Fig. 6b), the Mössbauer spectrum had a doublet and distributed hyperfine magnetic fields (DHMF) and contained α-Fe and γ-Fe. The intensity of the γ-Fe singlet became very low. The Mössbauer spectrum of a film

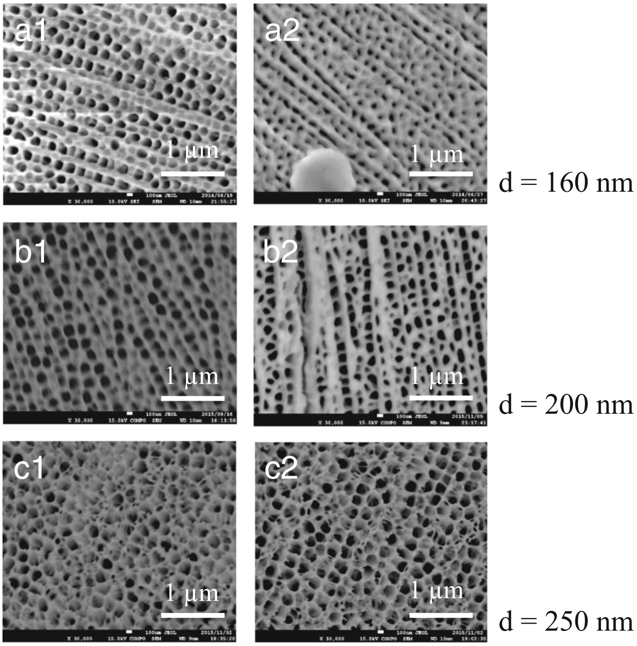

Fig. 4 SEM images of porous alumina substrates (**a1**, **b1**, and **c1**) and iron films deposited on them (**a2**, **b2**, and **c2**)

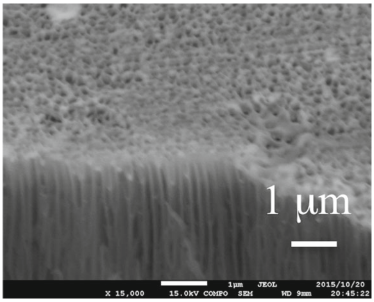

Fig. 5 SEM image of a cross section of an iron film deposited on porous alumina (pores with a diameter of 160 nm)

produced on porous alumina with the largest pore size (250 nm; Fig. 6c) was fitted to a combination of a doublet, a sextet, and a component of distributed hyperfine magnetic fields, as well as a very small amount of γ-Fe.

The distributed hyperfine magnetic fields (the mode at $H = 24$ T) can be attributed to large defects or a rough α-Fe lattice surface. The surface of the porous alumina does not have any planar regions, so iron atoms deposited on the rough surface could not form a long-range α-Fe lattice, resulting in distributed small hyperfine magnetic fields. It has been reported that the Mössbauer spectra of sonochemically prepared amorphous iron exhibited a broad sextet with an average magnetic hyperfine field of 25.9 T at 295 K [13]. The DHMF components in our Mössbauer spectra were assigned to iron containing large defects or amorphous iron.

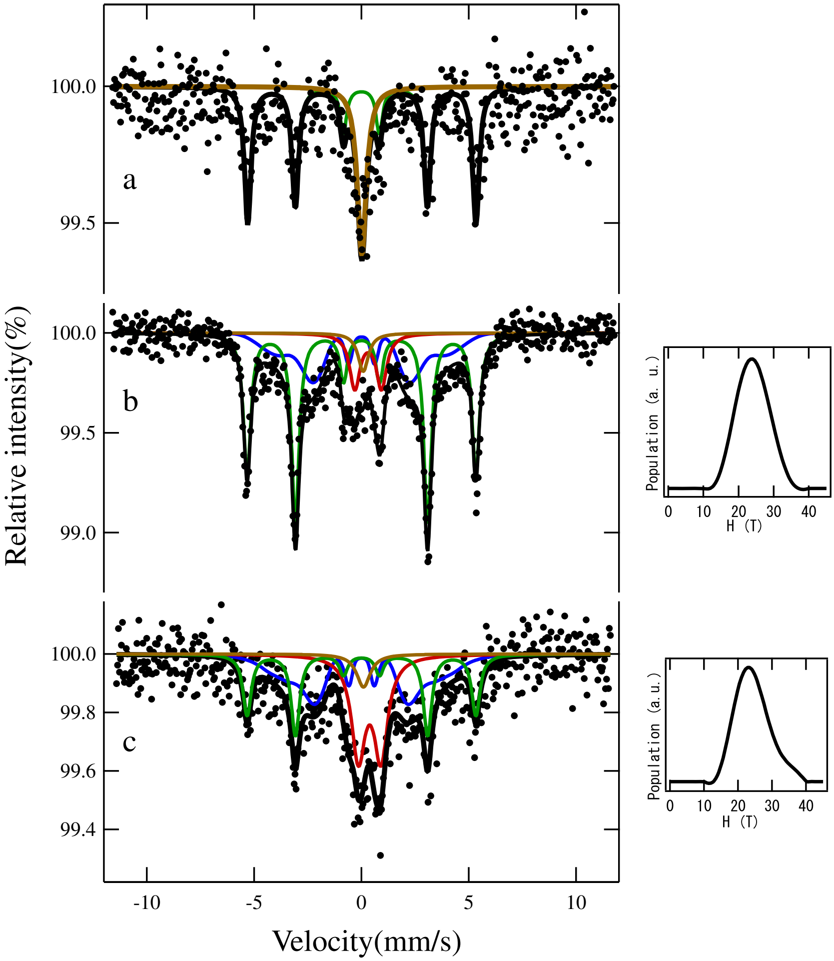

Fig. 6 Mössbauer spectra of iron films deposited on porous alumina substrates with different pore sizes. The diameters of the pores were (**a**) 160 nm, (**b**) 200 nm, and (**c**) 250 nm. The distributions of the hyperfine magnetic fields of the broad absorptions are indicated on the right side

The doublet ($\delta = 0.31$ mm/s, $\Delta E_q = 1.24$ mm/s) component was assigned to Fe^{3+} because of the isomer shift. The iron films with a rough morphology had large surface areas and contained many defects that reacted with oxygen relatively easily during handling in ambient atmosphere. The doublet component could be superparamagnetic iron oxide. The magnetic properties of hematite α-Fe_2O_3 nanoparticles have been studied [14], and the Mössbauer spectrum of a 16 nm particle showed a superparamagnetic doublet at room temperature. However, the ΔE_q value in our experiment was too large to assign it to α-Fe_2O_3 nanoparticles. The doublet had a relatively large ΔE_q value, which was assigned to paramagnetic high-spin Fe^{3+} in $Fe_xAl_{2-x}O_3$ reported in literature [15, 16]. The Al_2O_3 with large defects incorporated with Fe atoms to form $Fe_xAl_{2-x}O_3$.

Bulk γ-Fe is normally unstable at room temperature, but it is stabilized in nanometer-scale systems. In the present experiments, Fe atoms penetrated into small pores (less than

Table 1 Mössbauer parameters of the spectra shown in Fig. 6

Sample		δmm/s	ΔE_Qmm/s	HT	Γmm/s	Area int. %
a	$\alpha-$Fe	0.00(2)	0.00(4)	33.2(4)	0.50(2)	72
	$\gamma-$Fe	0.01(2)			0.36(3)	28
b	$\alpha-$Fe	0.00	0.00	33.0	0.42(2)	57
	$\gamma-$Fe	0.08(5)			0.58(7)	4
	Fe^{3+}	0.31(3)	1.24(5)		0.58(7)	11
	DHMF	0.00	0.00	24.0*		28
c	$\alpha-$Fe	0.00	0.00	33.0	0.55(7)	30
	$\gamma-$Fe	0.09(20)			0.78(12)	5
	Fe^{3+}	0.38(3)	1.05(9)		0.78(12)	31
	DHMF	0.00	0.00	24.0*		34

*Hyperfine magnetic field at the mode of the distribution

160 nm in diameter) to form a γ-Fe lattice and Fe atoms migrated over a long range to form α-Fe on the flat surface regions. When the pore diameter exceeded 200 nm, there was no flat surface region to produce a long-range ordered α-Fe lattice, nor were there small pores to stabilize the γ-Fe. These films had a rough surface, and α-Fe produced on a rough surface contained large defects. The defects or low crystallinity resulted in a distributed hyperfine magnetic field with a lower H value than that of bulk α-Fe (33T). When α-Fe with a rough surface is handled in atmosphere, α-Fe easily oxidizes to form iron oxides. Iron oxides supported in a nanoscale mixture with alumina (Al_2O_3) might be produced, as the porous alumina with larger pores were ready to incorporate Fe atoms in defects.

4 Conclusions

It was demonstrated that the surface morphology, especially the pore size, changed the composition of deposited iron films. γ-Fe was stabilized in small pores (less than 160 nm in diameter). γ-Fe was produced only inside the pores, and α-Fe covered the pores or the planar regions of the substrate surface to form a smooth surface when increasing the iron film thickness. When the pore diameter became larger than 200 nm, γ-Fe yield became very small instead, α-Fe was obtained, but it contained a large number of defects. The α-Fe showed smaller hyperfine magnetic fields. The Fe^{3+} component attributed to $Fe_xAl_{2-x}O_3$ was observed in iron films deposited on porous alumina with larger pores.

References

1. Yamada, Y., Kato, H., Kouno, K., Yoshida, H., Kobayashi, Y.: Iron films produced by an arc plasma gun. Hyperfine Interact **191**, 121–127 (2009)
2. Yasuike, M., Usui, R., Yamada, Y., Kobayashi, Y.: Orientation of hyperfine magnetic fields of α-iron films produced by laser deposition. Hyperfine Interact **205**, 23–26 (2012)
3. Thompson, G.E.: Porous anodic alumina: Fabrication, characterization and applications. Thin Solid Films **297**, 192–201 (1997)
4. Kalska-Szostko, B., Brancewicz, E.: Electrochemical deposition of nanowires in porous alumina. Acta Physica Polonica A **115**, 542–544 (2009)

5. Jagminas, A., Mažeika, K., Juška, E., Reklaitis, J., Baltrūnas, D.: Electrochemical fabrication and characterization of lepidocrocite (γ-FeOOH) nanowire arrays. Appl. Surf. Sci. **256**, 3993–3996 (2010)
6. Shi, Z., Zhang, Z., Fan, R., Gao, M., Guo, J.: Synthesis and characterization of iron particles hosted in porous alumina. J. Inorg. Organomet. Polym. **21**, 836–840 (2011)
7. Haneda, K., Zhou, Z.X., Morrish, A.H., Majima, T., Miyahara, T.: Low-temperature stable nanometer-size fcc-Fe particles with no magnetic ordering. Phys. Rev. B (Condensed Matter) **46**, 13832–13837 (1992)
8. Keune, W., Halbauer, R., Gonser, U., Lauer, J., Williamson, D.L.: Antiferromagnetism of fcc Fe thin films. J. Appl. Phys. **48**, 2976–2979 (1977)
9. Keune, W., Ezawa, T., Macedo, W., Glos, U.: Magneto-volume effects in γ-Fe ultrathin films and small particles. Physica B **161**, 269–275 (1990)
10. Preston, R.S., Gerlach, R.: Mössbauer effect in dilute alloys of iron in aluminum. Phys. Rev. B **3**, 1519–1526 (1971)
11. Yamada, Y., Namiki, K.: Spin orientation of iron films produced by laser deposition. Chem. Lett. **36**, 294–295 (2007)
12. Xu, Y., Yamazaki, M., Villars, P.: Inorganic materials database for exploring the nature of material. Jpn. J. Appl. Phys. **50**, 11RH02-1-5 (2011)
13. Long, G.J., Hautot, D., Pankhurst, Q.A., Vandormael, D., Grandjean, F., Gaspard, J.P., Briois, V., Hyeon, T., Suslick, K.S.: Mössbauer-effect and x-ray-absorption spectral study of sonochemically prepared amorphous iron. Phys. Rev. B **57**, 10715–10722 (1998)
14. Bødker, F., Hansen, M.F., Koch, C.B., Lefmann, K., Mørup, S.: Magnetic properties of hematite nanoparticles. Phys. Rev. B (Condensed Matter Mater. Phys.) **61**, 6826–6838 (2000)
15. Maksimov, Y.V., Tsodikov, M.V., Trusova, E.A., Suzdalev, I.P., Navío, J.A.: Origin of rate bistability in Mn–O/Al_2O_3 catalysts for carbon monoxide oxidation: Role of the Jahn–Teller effect. Catal. Lett. **72**, 11–15 (2001)
16. Tsodikov, M.V., Kugel, V.Y., Maksimov, Y.V., Ellert, O.G., Schcherbakov, V.M., Bukhtenko, O.V.: Iron-aluminum cluster catalysts obtained by alkoxy synthesis.: 1. Liquid-phase oxidation of hexadecane. J. Catal. **148**, 113–118 (1994)